

UNCLASSIFIED

AD NUMBER

AD802189

LIMITATION CHANGES

TO:

Approved for public release; distribution is unlimited.

FROM:

Distribution authorized to U.S. Gov't. agencies and their contractors; Critical Technology; 12 OCT 1966. Other requests shall be referred to Air Force Office of Scientific Research, Attn: SRGL, 1400 Wilson Boulevard, Arlington, VA 22209. This document contains export-controlled technical data.

AUTHORITY

AFOSR ltr dtd 12 Nov 1971

THIS PAGE IS UNCLASSIFIED



9  
October 12, 1966

802189

Quarterly Report No. 3

1 July - 30 September, 1966

RESPONSE OF A BURNING PROPELLANT SURFACE TO EROSION TRANSIENTS

By: E. L. Capener  
L. A. Dickinson  
G. A. Marxman  
C. E. Wooldridge

Prepared for:

AIR FORCE OFFICE OF SCIENTIFIC RESEARCH  
WASHINGTON, D.C. 20333

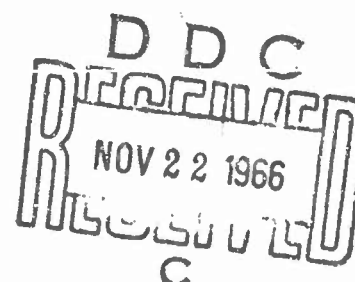
SRI Project No. FRU-5818

Contract No. AF 49(638)-1665

Approved:

*Lionel A. Dickinson*

Lionel A. Dickinson, Director  
Polymer & Propulsion Sciences Division



Copy No. 25

## CONTENTS

---

	Page
LIST OF ILLUSTRATIONS . . . . .	111
INTRODUCTION . . . . .	1
THEORETICAL INTERPRETATION OF EXPERIMENTAL RESULTS . . . . .	2
Traveling Wave Phenomena . . . . .	2
Tubular Motor Results . . . . .	6
INTERACTION OF THE TRAVELING WAVE AND THE COMBUSTION MECHANISM . . . . .	11
Local Frequency of the Pressure Pulse Caused by the Passing Shock Wave . . . . .	12
Theoretical Frequency Response of the Propellant Combustion Mechanism . . . . .	13
The Influence of Surface-Coupled Reactions . . . . .	20
Summary . . . . .	20

## ILLUSTRATIONS

		Page
Fig. 1	Traveling Wave Instability in a Slab Burner . . . . .	3
Fig. 2	Schematic Evolution of the Shock-Expansion Process During Longitudinal Instability . . . . .	4
Fig. 3	Head-End Pressure Transients During Traveling Wave Instability in a Tubular Burner . . . . .	7,8
Fig. 4	Amplitude of Steady-Oscillatory Mode for $\Theta_g = 0.5$ . . . . .	15
Fig. 5	Influence of Burning Rate and Composition on Finite Amplitude Traveling Wave Instability; Solid Line, Stable Regime; Dotted Line, Unstable Regime; for 5-Inch x 40-Inch Motor . . . . .	19

## TABLES /

Table I	Tubular Motor Instability Data . . . . .	9
Table II	Frequency of Pressure Pulse, CPS . . . . .	13
Table III	Approximate Resonant-Frequency Range For a Typical Composite Propellant According to Theoretical Combustion Model . . . . .	17

## INTRODUCTION

During this quarter our efforts have been directed toward integrating the propellant response model with the experimental results in a more basic way.

A gas dynamic study has shown that the finite amplitude traveling wave can be sustained in a combustion chamber by a modest input of energy--1% to 3% of the combustion energy; the source of this energy might be easily explained by partially completed reactions at the surface. However, the fact that there are certain limits to the frequency at which instability occurs suggests that gas phase perturbations respond to reactions with a relatively long relaxation time. The analytical study has revealed that a large response is associated with a significant fractional heat release (for composite propellants) occurring in the condensed phase or surface-coupled reactions. In the experimental study, attempts are being made to identify the nature of solid phase reactions and to differentiate between condensed phase and gas phase reactions. Adiabatic self-heating studies and differential thermal analysis studies are being performed at a range of pressures.

Preliminary experimental results suggest that between 10% and 20% of the heat release occurs in the solid phase reactions of certain AP-based propellants; the condensed phase heat release for KP-based propellants appears to be much less.

Using activation energies obtained in experimental studies previously reported in this program, it has proved possible to theoretically predict the frequency band for propellant response. The magnitude of this response is dependent on the heat release in the solid (condensed) phase. The frequency band predicted agrees closely with the preferred frequencies experimentally observed. This appears to represent a significant advance in theoretical prediction of unstable combustion characteristics from ballistic data (burning rate) and physical chemical data (activation energy).

## THEORETICAL INTERPRETATION OF EXPERIMENTAL RESULTS

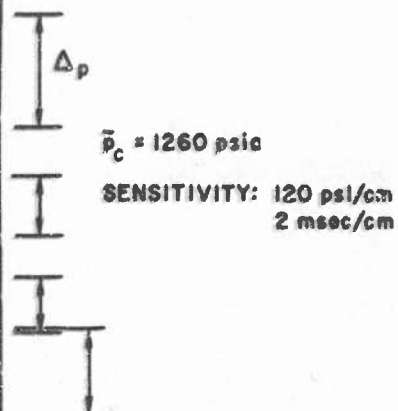
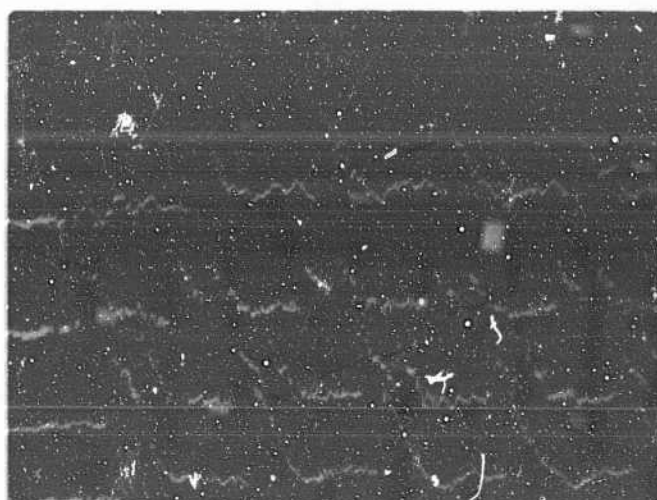
### Traveling Wave Phenomena

During the past quarter attention has been focused on the behavior of traveling waves in the combustion chamber, and especially upon further interpretation of the available data. Typical experimental behavior is shown in Figure 1 for PBAN 319 propellant in a slab motor operating at a mean pressure of 1260 psia. The important points to be noted are that the head-end and aft-end pressure pulses are nearly equal in magnitude and approximately twice as large as the pulses measured at the one-quarter and three-quarter length stations. The aft-end pulse is slightly smaller than the head-end pulse, presumably because of some energy loss upon reflection from the open nozzle.

From a phenomenological point of view, the behavior illustrated by the pressure traces of Figure 1 can be explained by the presence of a constant strength shock-expansion process which is traveling back and forth in the motor. The passage of the shock wave past any point induces a particle velocity behind it in the direction of travel of the shock, as well as pressure and temperature jumps. In order to satisfy the continuity equation, an expansion process which reduces the induced velocity to zero must form behind the shock wave, as shown schematically in Figure 2. Since the expansion process is isentropic, the local velocity of the expansion field will be the local speed of sound which decreases with increasing distance behind the shock wave. Thus the extent of the expansion process will lengthen as wave travel proceeds down the chamber.

When the shock wave reflects from the end of the chamber, the measured perturbation amplitude doubles because the shock wave will maintain the same pressure change across itself, whereas the pressure in front of the reflected shock is the pressure which was behind the





TA-5918-15

FIG. 1 TRAVELING WAVE INSTABILITY IN A SLAB BURNER

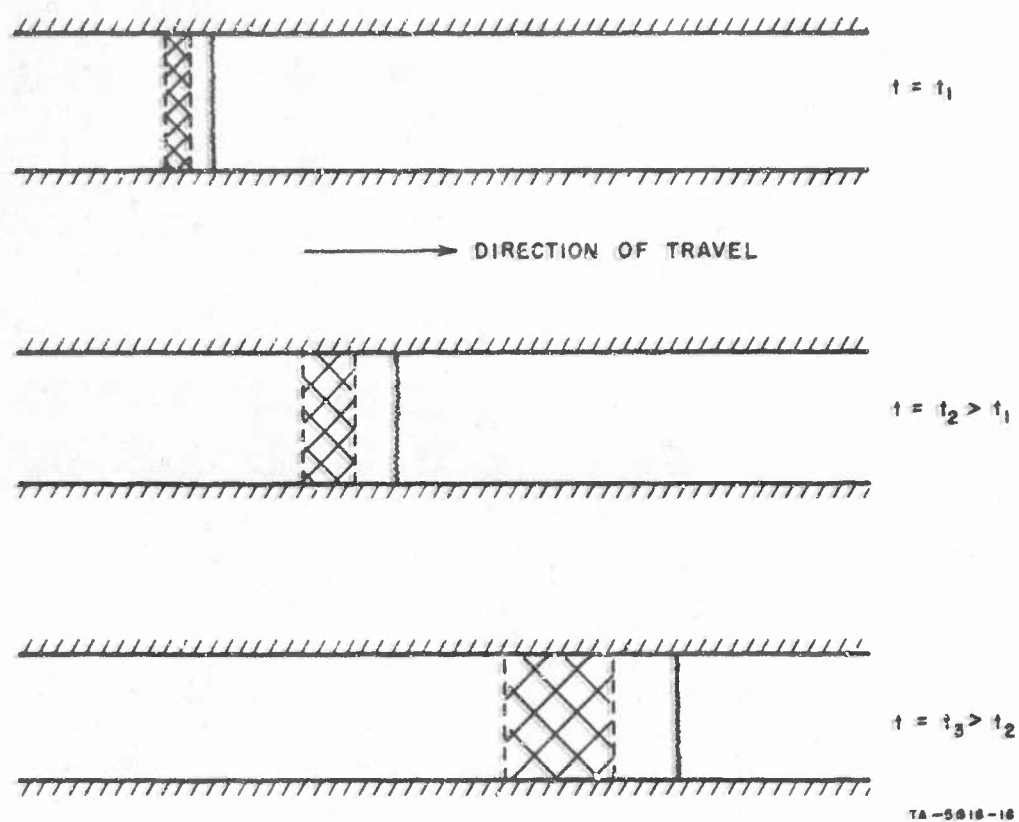


FIG. 2 SCHEMATIC EVOLUTION OF THE SHOCK-EXPANSION PROCESS DURING LONGITUDINAL INSTABILITY



incident shock. A correspondingly strong expansion process will follow the reflected shock back down the passage toward the oncoming expansion process which was following the incident shock. This incoming expansion process reduces the strength of both the reflected shock and its trailing expansion process down to the strengths of the original process and the chain of events is repeated in the opposite direction. This complicated turn-around process occurs in a very short physical distance, making the details very difficult to obtain experimentally.

This physical reasoning is borne out by further examination of Figure 1. Not only does pressure-doubling occur at the ends, but the wave velocity along the chamber is nearly constant, since a comparison of the data at the quarter-length point with that at the head-end shows that about one-quarter of the total wave travel time is used over the first quarter of the motor. A constant wave velocity implies a constant wave strength; within the accuracy of the traces, the strengths at the one-quarter and three-quarter points are the same.

The final strength (and therefore velocity) of the wave will be determined by the balance between the energy input process and the dissipation process at the walls and by the coupling between the passage of the wave and the primary combustion process. This latter coupling is discussed in detail in a later section. A possible mechanism for the local input of energy into the traveling wave is the heat release from gas-phase reactions which are induced by the temperature jump across the shock wave.

If the traveling wave is considered as a Chapman-Jouget detonation, the pressure perturbation is related to the Mach number and the pressure ahead of the shock by

$$\frac{\Delta p}{p_1} = \frac{\gamma}{\gamma + 1} (M^2 - 1) \quad (1)$$

and the heat release required to drive the wave is

$$\frac{Q}{c_p T_1} = \frac{(M - 1)^2}{2(\gamma + 1)M^2} \quad (2)$$

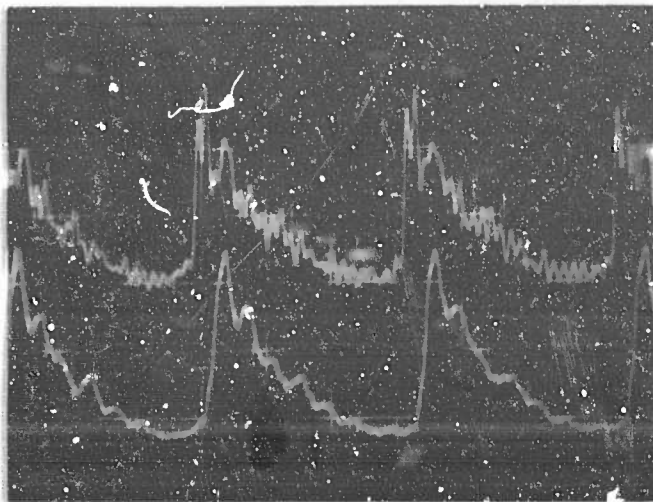
For the data of Figure 1,  $\Delta p/p_1 \approx 0.093$  giving  $M \approx 1.08$  and  $Q/c_p T_1 \approx 1.25 \times 10^{-4}$ . Since  $c_p T_1$  is of the order of the available energy per unit mass of the propellant, it is clear that only a small fraction of this available energy is required to drive the shock wave. It must be noted that the above calculation does not account for energy lost in dissipation at the walls, so that the actual  $Q$  extracted from the stream is larger than the value calculated above. Since the dissipation might be expected to be less in a tubular burner than in a slab burner, energy should be available to drive a stronger wave in a tubular burner. That this is indeed the case is shown below.

To summarize, traveling wave data obtained in a slab burner supports the concept of the instability being a constant strength detonation wave supported by an energy input from gas phase reactions which is small compared to the total energy available in the propellant. More important is the coupling between the wave process and the main combustion process which is discussed in detail below.

#### Tubular Motor Results

Head-end pressure measurements obtained in tubular motors with five different propellants are shown in Figure 3. Two traces are shown for each propellant, the lower one of which has been filtered to remove the organ pipe oscillation in the small cylindrical chamber ahead of the transducer. Results are given in Table I.

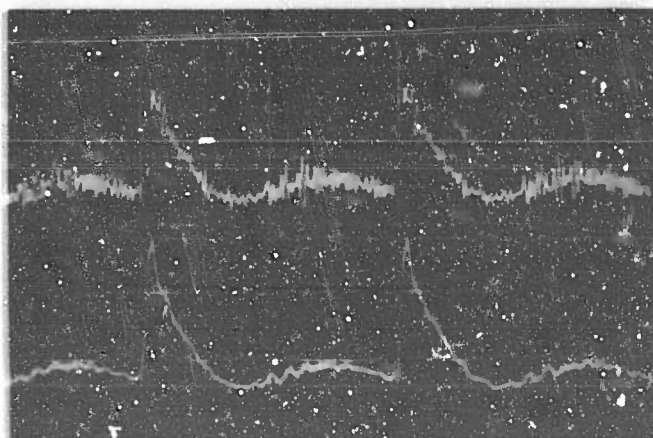
The wave amplitude (see Table I), computed as half the head-end pressure pulse for reasons discussed above, is relatively constant for all the propellants considered, being about  $\Delta p/\bar{p} = 0.17$ . The variations which do occur undoubtedly depend more upon the ratio of the mean pressure to the threshold pressure for instability than upon compositional factors in these similar AP-based propellants. Using this value for  $\Delta p/\bar{p}$ , and assuming that  $p = \bar{p} - (\Delta p/2)$ , equation (1) gives  $M \approx 1.2$  for the



PBAN 1103

$\bar{p}_c = 915$  psia

SENSITIVITY: 120 psi/cm  
0.5 msec/cm



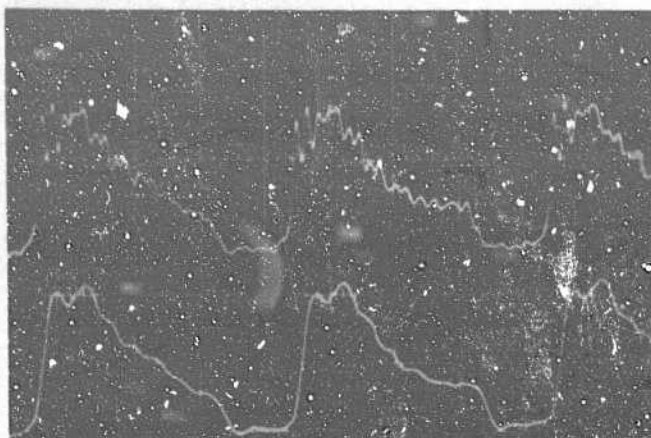
PBAN 1104

$\bar{p}_c = 565$  psia

SENSITIVITY: 80 psi/cm  
0.5 msec/cm

TA-5016-16

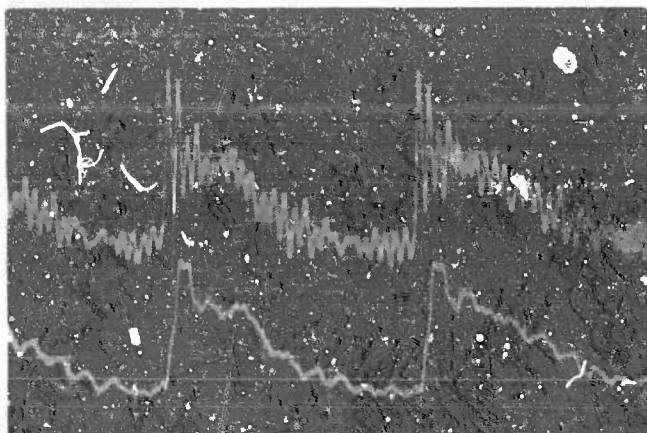
FIG. 3 HEAD-END PRESSURE TRANSIENTS DURING TRAVELING WAVE INSTABILITY IN A TUBULAR BURNER



PBAN 244

$\bar{p}_c = 410$  psia

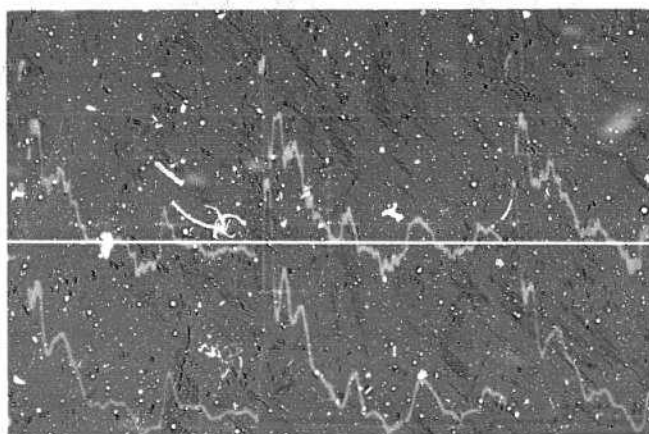
SENSITIVITY: 60 psi/cm  
0.5 msec/cm



PBAN 284

$\bar{p}_c = 535$  psia

SENSITIVITY: 80 psi/cm  
0.5 msec/cm



PBAN 31S

$\bar{p}_c = 1215$  psia

SENSITIVITY: 120 psi/cm  
1 msec/cm

7A-5816-17

FIG. 3 (Continued)

TABLE I  
TUBULAR MOTOR INSTABILITY DATA

Propellant	Composition	Motor Length (inches)	Wave Amplitude ( $\Delta p/\bar{p}$ )	Wave Frequency (cps)
PBAN 103	24% ground* } $\text{NH}_4\text{ClO}_4$ 56% unground } 20% PBAN	40	0.185	600
PBAN 104	22.5% ground* } $\text{NH}_4\text{ClO}_4$ 56% unground } 20% PBAN 1.5% LiF	82	0.169	244
PBAN 244	27% ground* } $\text{NH}_4\text{ClO}_4$ 52% unground } 20% PBAN 1% LiF	40	0.163	500
PBAN 284	20% - 20 $\mu$ } $\text{NH}_4\text{ClO}_4$ 20% - 600 $\mu$ } 39.5% unground } 20% PBAN 0.5% $\text{SrCO}_3$	40	0.138	513
PBAN 319	22% - 20 $\mu$ } $\text{NH}_4\text{ClO}_4$ 22% - 600 $\mu$ } 34% unground } 17% PBAN 5% Al	82	0.184	250

\*Average particle diameter of 10 $\mu$ .



wave Mach number and equation (2) gives  $Q/c_p/T_1 \approx 6.3 \times 10^{-3}$ . Even accounting for dissipation, it conservatively appears that less than 2 percent of the propellant energy is needed for direct input to the wave. Notice that the dissipation is much smaller in the tubular burner than in the slab burner.



## INTERACTION OF THE TRAVELING WAVE AND THE COMBUSTION MECHANISM

As has been well-documented in this program and others, axial-mode combustion instability arises when conditions are such that a pressure disturbance does not decay, but instead develops into a traveling wave reflecting back and forth between the ends of the chamber. The preceding discussion shows that this wave is actually a weak shock wave; its strength depends to some degree on the propellant formulation and chamber conditions, but is almost independent of axial position in the chamber. Usually, the Mach number of this traveling shock wave is approximately 1.2.

The energy feedback from the reaction zone required to maintain a shock of this strength represents only about 2 percent of the total rate of energy release in the typical propellant combustion process. This observation leads to a very important conclusion; it is unlikely that the appearance of axial-mode instability is governed primarily by the amount of energy feedback from the combustion process to the traveling wave, since so little energy is needed to support the wave. Of course, the energy flux magnitude does play a significant role, particularly in a motor with a high damping factor, or high losses. However, it is likely that a more important factor in determining the axial-mode stability characteristics of a solid rocket motor is the phase relationship between the energy feedback at any given point on the propellant, and the passage of the wave over that point. In other words, if the energy feedback (or mass-flux perturbation at the surface, which is essentially equivalent) is locally in phase with the passing shock wave over most of the burning surface, the shock wave will be reinforced and instability will result. If the two events are locally out of phase over most of the length of the grain, the shock wave will decay and stable combustion will be achieved. This phase relationship is determined by the combustion chamber length and by the frequency response characteristics of the combustion mechanism.

### Local Frequency of the Pressure Pulse Caused by the Passing Shock Wave

As the shock wave travels axially back and forth in the combustion chamber, it creates an oscillatory pressure disturbance at every point on the propellant surface. The frequency of this disturbance at any given axial position corresponds to the number of times per second that the wave passes this position. In general, there are two distinct frequencies associated with any given axial position. One of these corresponds to the time required for a shock wave which is traveling toward the right, to be reflected from the right end of the chamber and return to the reference point. The other frequency corresponds to the time for a wave traveling toward the left end to be reflected and return to the same point. At the ends of the chamber only one of these frequencies pertains (i.e., the other is infinite); at the center they are equal, of course. From a brief consideration of this phenomenon one can readily show that the pulse frequency at the center of the chamber is exactly twice that at the ends. At intermediate stations the propellant is subjected to a train of pulse pairs. For example, at one-quarter and three-quarter positions the separation between pairs corresponds to a recurrence frequency of two-thirds of that at the center, while the spacing between two pulses in a pair corresponds to a frequency of twice that at the center. The band of frequencies encountered is dependent on the motor length and the motor surface is dependent on the net driving and damping of the wave train.

Pulse frequencies encountered in experiments performed during this program<sup>1</sup> are shown in Table II.

For the 23-, 40-, and 82-inch motors, frequencies were measured at the head-end pressure transducer. As was shown in earlier discussion in this report, these frequencies are produced by a traveling shock wave moving at  $M = 1.2$  back and forth in the chamber. Ordinarily, pulses introduced in the 15-inch motor were found to decay, i.e., with most propellants this motor could not be driven to unstable combustion. The frequencies shown in Table II for this motor are the calculated

---

<sup>1</sup>Capener, E. L., R. J. Kier, L. A. Dickinson, and G. A. Marxman, Response of a Burning Propellant Surface to Erosive Transients, Final Scientific Report, A.F. Office of Scientific Research Contract AF 49(638)-1507, March 15, 1966.

TABLE II  
FREQUENCY OF PRESSURE PULSE, CPS

Length of Chamber, inches	End	Axial Position		Center
		1/4 L	3/4 L	
15	1240	1660	4960	2480
23	803	1070	3212	1606
40	465	620	1860	930
82	238	318	952	476

characteristic frequencies based on a traveling shock wave with  $M = 1.2$ . Also, it is important to note that in some cases the 82" motor tended to go unstable in a double mode, i.e. with traveling waves in two 41" sections reflecting against each other at the center. In this case the frequencies for the 82" motor are essentially the same as for the 40" motor, where the center of the longer motor acts as the "end" of two shorter ones.

#### Theoretical Frequency Response of the Propellant Combustion Mechanism

As a first step toward explaining our experimentally determined limits of axial-mode combustion instability,<sup>1</sup> it is essential to compare the observed frequency characteristics, as reported in Table I, with the frequency response characteristics of the propellant combustion mechanism. The latter has been predicted by the theoretical combustion model developed in earlier reports.<sup>1,2,3</sup> Thus, an attempt to explain

<sup>2</sup>Capener, E. L., L. A. Dickinson, and G. A. Marxman, Response of a Burning Propellant Surface to Erosive Transients, First Quarterly Report, Air Force Office of Scientific Research, Contract No. AF 49(638)-1665, April 1966.

<sup>3</sup>Capener, E. L., L. A. Dickinson, and G. A. Marxman, Response of a Burning Propellant Surface to Erosive Transients, Second Quarterly Report, Air Force Office of Scientific Research, Contract No. AF 49(638)-1665, July 1966.

observed instability characteristics in terms of the analytical predictions affords a significant test of the underlying theoretical concepts.

As a specific example, Figure 4 shows the theoretical frequency-response characteristic of a composite propellant in which about 5 percent of the total heat release occurs in surface-coupled reactions, and the rest occurs in the usual gas-phase reactions. This figure is reproduced from an earlier report,<sup>2</sup> wherein its basis is described. The coordinates are composed of groupings of thermo-chemical parameters of the propellant. Thus, any propellant, having certain values of the activation energies, surface temperature, etc., can be represented as a point of Fig. 1. The solid curves show the maximum ratio of burning rate oscillation amplitude to pressure disturbance amplitude that can occur at any given point. Only a certain frequency of pressure disturbance (shown by the dashed curves) can induce that response. Any other frequency of pressure oscillation causes a smaller-amplitude burning-rate oscillation.

The first thing to note about Fig. 4 is that the frequency at which the propellant responds most strongly depends almost entirely on the value of  $A$  (i.e. the dashed curves are nearly horizontal). This is even more true at higher values of  $\theta_s$  (greater percentages of surface-coupled heat release) than that associated with Fig. 1. Thus, the resonant frequency of the combustion mechanism,  $f = \omega/2\pi$ , depends on the burning rate  $\bar{r}$ , the thermal diffusivity of the solid  $K$ , and also on the activation energy of surface decomposition  $E$  as well as the surface temperature.

The other important point shown by Fig. 4 is that the maximum amplitude of the burning rate oscillation, as represented by the amplification factor  $\tilde{r}/\tilde{p}$ , depends almost entirely on the value of  $\alpha$  associated with that propellant. (This is not true at low values of  $A$ , but few actual propellants fall in that range.) Thus the maximum possible amplification factor for a given propellant is determined largely by the activation energy of the gas-phase flame  $E_f$ , the gas-phase flame temperature  $T_f$ , and the effective overall order  $n$  of the gas-phase reactions.



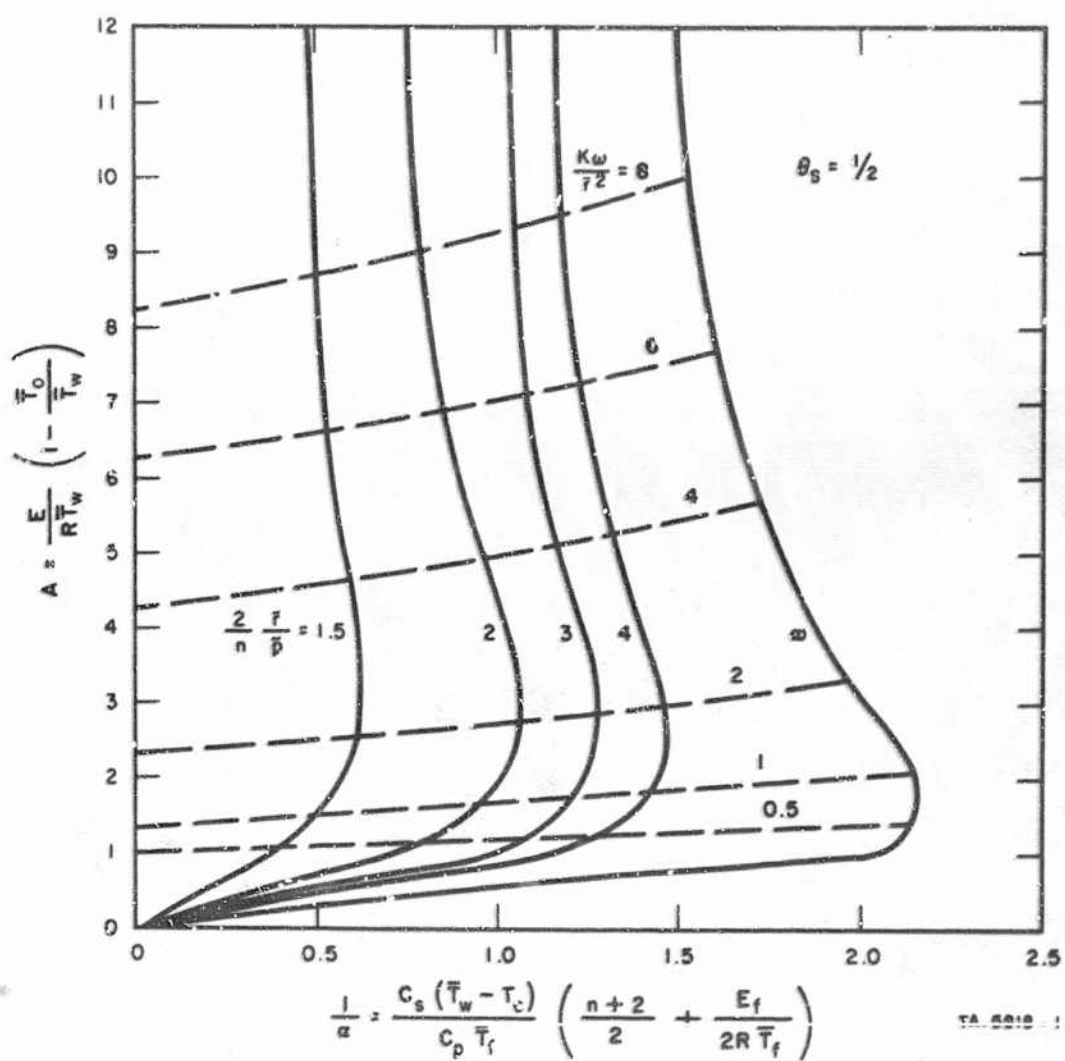


FIG. 4 AMPLITUDE OF STEADY-OSCILLATORY MODE FOR  $\theta_S = 0.5$

However, there is a third important point that cannot be deduced from Fig. 4 alone; the amplitude of the burning rate response is also strongly influenced by  $\Theta_s$ . It can be shown<sup>2</sup> that as  $\Theta_s$  increases (increasing percentage of surface-coupled heat release) the solid curves move toward the left, and the "bump" in these curves in the region  $1 < A < 3$  is eliminated. (This occurs rapidly; the bump is gone at  $\Theta_s = 1.0$ ). This means that of two propellants with similar values of the thermochemical parameters (and, therefore, the values of  $A$  and  $\alpha$ ), the one with more surface-coupled heat release (greater  $\Theta_s$ ) will have a higher amplitude burning-rate oscillation for a given pressure oscillation. Inasmuch as most propellants probably have similar values of  $\alpha$ , this effect may be a key factor in separating those that burn stably from those that do not.

To put these theoretical conclusions in a more quantitative form it is necessary to assign approximate values to the thermochemical parameters that characterize the propellants. For most composite propellants it is reasonable to assume that the activation energy for surface decomposition is  $E_s \approx 30$  kcal. The surface temperature  $T_w$  is approximately  $800^\circ\text{K}$ , and the gas-phase flame temperature  $T_f \approx 2500^\circ\text{K}$ . The activation energy for the gas-phase flame usually is  $E_f \approx 20$  kcal and the overall effective order of that reaction  $n$  is about 2. The parameters for a very wide range of propellants, including those that have been investigated experimentally in this program, almost certainly fall within 20% of these figures. Thus, a typical composite propellant is characterized in Fig. 4 by the coordinates  $A \sim 10$ ,  $1/\alpha \sim 1$ . It follows from the theory (Fig. 4) that the resonant frequency  $f$  of the combustion mechanism for such propellants corresponds to  $K_w/\bar{r}^2 \sim 9$ , or  $f \sim 9\bar{r}^2/2\pi K$ . It also can be shown that the maximum deviation from this frequency for which there is a significant burning-rate amplification is about:

$$\Delta f \sim \pm 2\bar{r}^2/2\pi K$$



(This frequency range follows directly from an examination of the mathematical analysis and may be deduced by referring to the mathematically similar treatment by Denison and Baum.<sup>4</sup>) A typical thermal diffusivity for solid propellants is  $K \approx 2.3 \times 10^{-4} \text{ in}^2/\text{sec}$ . Accordingly, the approximate frequency range in which the combustion mechanism tends to amplify a pressure oscillation is as indicated in Table III. The frequency given in the table is the approximate resonance frequency, or point of maximum amplitude, and the tolerance figures indicate the approximate range in which a degree of amplification is present.

TABLE III  
APPROXIMATE RESONANT-FREQUENCY RANGE FOR A  
TYPICAL COMPOSITE PROPELLANT ACCORDING TO THEORETICAL COMBUSTION MODEL

$\bar{r}$ (in/sec)	$f$ (cps)
0.1	$\sim 60 \pm 15$
0.2	$\sim 250 \pm 80$
0.3	$\sim 560 \pm 130$
0.4	$\sim 1000 \pm 210$
0.5	$\sim 1550 \pm 340$

It is reasonable to assume that axial-mode combustion instability may arise in a solid rocket chamber whenever an appreciable portion of the grain length is subjected to pressure oscillations near the resonance frequency of the combustion mechanism. On this basis a comparison of Tables II and III afford some interesting conclusions.

In a 15-inch chamber, only a very high burning rate propellant should be susceptible to axial-mode instability. With a 0.5-inch/sec burning rate, only the portion of the propellant near the ends of the chamber can experience pressure oscillations in the resonance range. With lower burning rates, no part of the combustion surface is in resonance with the waves. Thus, with propellants in the normal burning rate range the theory predicts that combustion instability should be difficult to initiate (or rarely experienced) in a 15-inch chamber. This agrees with our experimental observations.

<sup>4</sup>M. R. Denison and E. Baum, "A Simplified Model of Unstable Burning in Solid Propellants," ARS Journal, 31, 1112 (1961).

Instability is much more likely in the 23-inch and 40-inch chambers. In the former, propellants with burning rates of 0.35 to 0.45 inch/sec should be particularly susceptible to instability. The corresponding range in the 40-inch chamber is about 0.2 to 0.4 inch/sec. The stability characteristics of a number of propellants have been thoroughly documented experimentally in a 40-inch chamber during this program.<sup>1</sup> The results are shown in Fig. 5. It is apparent that the burning rates of the propellants that encountered instability fell in the range 0.1 to 0.3 inch/sec. Though this range is somewhat lower than that predicted theoretically, the agreement is well within the tolerances imposed by uncertainties in evaluating the thermochemical constants of the propellant. The theoretically predicted resonance-frequency bounds offer a plausible explanation for the fact that the high burning rate AP/KP propellant was stable, whereas the other one was not. They may also explain why the KP, LiP, and AN propellants were stable, as all these have resonance frequencies well outside the wave frequencies typical of a 40-inch motor. However, there is also another factor that may be significant here--the value of  $\Theta_g$  which determines the amplitude of the burning rate response. This factor certainly appears to be important relative to the opposite behavior of the AN/KP and AN/AP propellants, which should have similar resonance frequencies. We shall consider this point further in later discussion.

In the 82-inch motor it was found experimentally that the shock wave traveled from end to end of the motor, with the frequencies shown in Table II, only during the first 100 msec after the initiating pulse. In every case the motor failed to sustain such a mode beyond this initial period. Instead, a transition to a double mode, or essentially the first harmonic, always occurred. In this case there were two traveling shock waves in the motor, each traveling through a 41-inch section and reflecting off the other wave at the center. Thus, the 82-inch motor always undergoes a transition to an axial instability mode that exhibits the same frequency range as that shown for a 40-inch motor in Table II. This is precisely what one would expect for this propellant (PBAN 103,  $\bar{r} \sim 0.25\text{--}0.3$  inch/sec) from

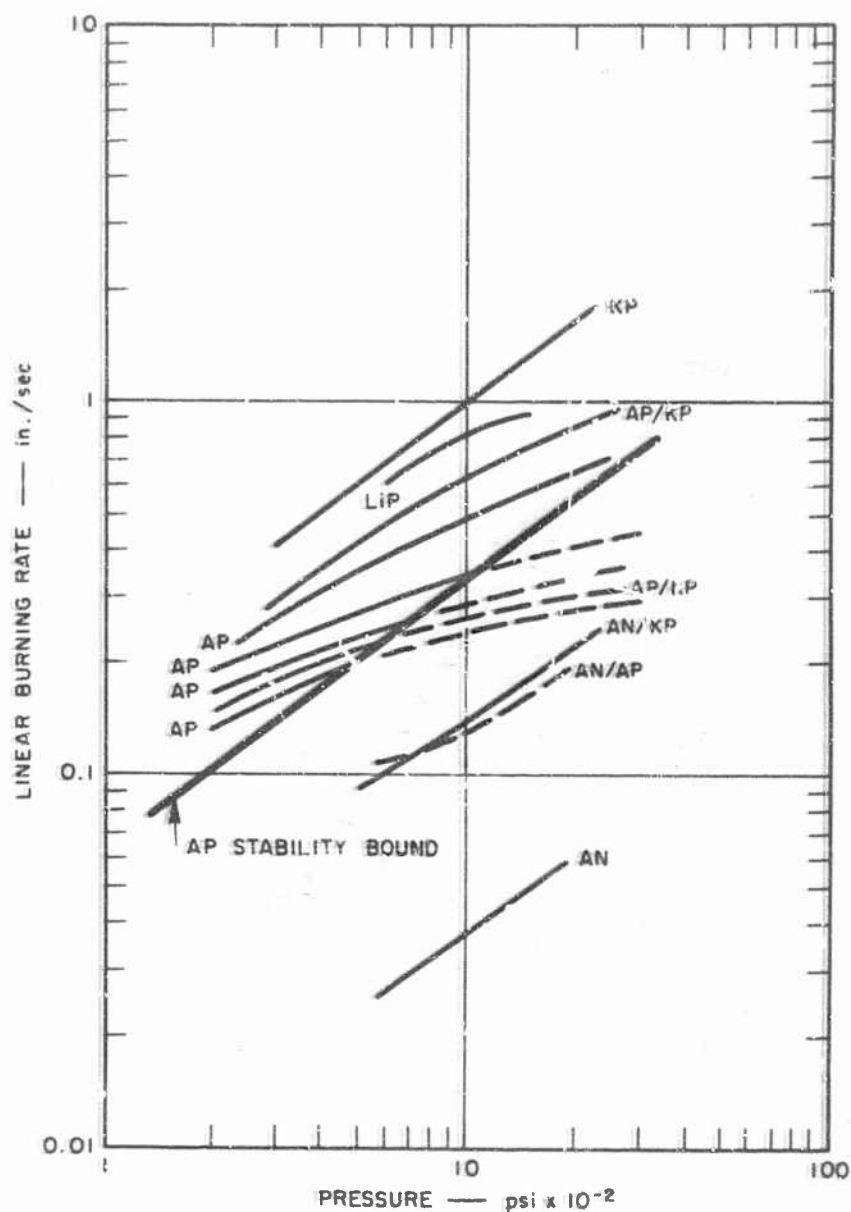


FIG. 5 INFLUENCE OF BURNING RATE AND COMPOSITION ON FINITE AMPLITUDE TRAVELING WAVE INSTABILITY; SOLID LINE STABLE REGIME, DOTTED LINE UNSTABLE REGIME FOR 5-INCH x 40-INCH MOTOR

the theoretical analysis of Table III. The fundamental mode of the 82-inch motor corresponds to a frequency range (Table II) that is somewhat below the resonance frequency-response range of the propellant. However, the double-wave mode, which corresponds to the frequencies of a 40-inch motor (Table I), is right in the resonance range, as has already been shown. Thus the transition to this mode in the longer motor is entirely consistent with the theoretical predictions.

#### The Influence of Surface-Coupled Reactions

The foregoing discussion deals only with the resonance-frequency aspect of the combustion model. To fully explain the data it is necessary to consider the remaining theoretical parameter  $\Theta_s$ , which is a measure of the surface-coupled heat release. In general, when  $\Theta_s$  is large for composite propellants (e.g. 10-20% of total energy release in surface-coupled reactions), the amplitude of the burning rate response in the resonance frequency range is large. When  $\Theta_s$  is small (10% or less heat release near the surface) the amplitude is greatly reduced, according to the theory. This affords a possible explanation for the behavior of the AN/KP and AN/AP propellants in Fig. 5. It has been shown during this program that AP decomposition and combustion is associated with a high surface exotherm, whereas the surface-coupled energy release is believed to be lower with KP. Thus, although both the AN/AP and the AN/KP propellants are in their resonant frequency range in the 40-inch motor, the former probably has a much stronger response. Consequently the normal damping phenomena in the motor cannot prevent the AP composition from going axially unstable, but they can do so with the KP propellant. In terms of Fig. 5, this means that the stability bound for the AN/KP propellant is approximately parallel to the AP bound shown, but has a lower intercept on the burning rate coordinates. This was derived from the theory previously.<sup>1</sup>

## SUMMARY

The theoretical combustion model affords a plausible, consistent, and comprehensive, though not proven, explanation for the experimentally observed axial-mode instability phenomena. Two factors enter: (1) the resonance frequency range of the combustion mechanism, and (2) the amplitude of the response in the range. The former depends primarily on the burning rate and also on thermochemical characteristics of the decomposition process (activation energy, surface temperature). It can be evaluated quantitatively with reasonable accuracy. The amplitude response depends primarily on the degree of surface-coupled heat release, and also on thermochemical parameters of the flame. As yet we do not know how to measure or accurately predict the surface-coupled reactions associated with a given propellant. Therefore, the amplitude factor is difficult to predict a priori, although experiments such as those reported in Fig. 5 are in a sense a measure of it. This is certainly an area that will require much more attention, both experimentally and theoretically.



Unclassified

Security Classification

DOCUMENT CONTROL DATA - R&D

(Security classification of title, body of abstract and indexing annotation must be entered when the overall report is classified)

1 ORIGINATING ACTIVITY (Corporate author) Stanford Research Institute 333 Ravenswood Avenue Menlo Park, California 94025		2a REPORT SECURITY CLASSIFICATION Unclassified	
		2b GROUP	
3 REPORT TITLE  RESPONSE OF A BURNING PROPELLANT SURFACE TO EROSION TRANSIENTS			
4 DESCRIPTIVE NOTES (Type of report and inclusive dates) Scientific <del>INTERIM</del> INTERIM			
5 AUTHOR(S) (Last name, first name, initial) Capener, Erwin L. Wooldridge, Charles E. Dickinson, Lionel A. Marxman, Gerald A.			
6 REPORT DATE October 12, 1966		7a. TOTAL NO. OF PAGES 24	7b. NO. OF REFS 4
8a. CONTRACT OR GRANT NO. 49(638)-1665		8a. ORIGINATOR'S REPORT NUMBER(S) FRU-5818	
8b. PROJECT NO. 9713-01			
c. 61445014			
d. 681308		9b. OTHER REPORT NO(S) (Any other numbers that may be assigned this report) <b>AFOSR 66-2483</b>	
10 AVAILABILITY/LIMITATION NOTICES  Subject to special export control and each transmittal to foreign governments or foreign nationals may be made only with prior approval of AFOSR(SRGL).			
11 SUPPLEMENTARY NOTES		12. SPONSORING MILITARY ACTIVITY AF Office of Scientific Research (SREP) 1400 Wilson Boulevard Arlington, Virginia 22209	

13 ABSTRACT

Theoretical analysis of the unstable behavior of solid propellants has permitted the propellant response (preferred frequencies) to be calculated in terms of burning rate and activation energies for solid and gas phase reactions.

The fractional heat release in the condensed phase reactions has been shown to be of importance in determining the magnitude of the propellant response.



Unclassified

Security Classification

KEY WORDS	LINK A		LINK B		LINK C	
	ROLE	WT	ROLE	WT	ROLE	WT
Solid Propellants						
Composite Propellants						
Propellant Response						
Solid Phase Reactions						

INSTRUCTIONS

1. **ORIGINATING ACTIVITY:** Enter the name and address of the contractor, subcontractor, grantee, Department of Defense activity or other organization (corporate author) issuing the report.

2a. **REPORT SECURITY CLASSIFICATION:** Enter the overall security classification of the report. Indicate whether "Restricted Data" is included. Marking is to be in accordance with appropriate security regulations.

2b. **GROUP:** Automatic downgrading is specified in DoD Directive 5200.10 and Armed Forces Industrial Manual. Enter the group number. Also, when applicable, show that optional markings have been used for Group 3 and Group 4 as authorized.

3. **REPORT TITLE:** Enter the complete report title in all capital letters. Titles in all cases should be unclassified. If a meaningful title cannot be selected without classification, show title classification in all capitals in parenthesis immediately following the title.

4. **DESCRIPTIVE NOTES:** If appropriate, enter the type of report, e.g., interim, progress, summary, annual, or final. Give the inclusive dates when a specific reporting period is covered.

5. **AUTHOR(S):** Enter the name(s) of author(s) as shown on or in the report. Enter last name, first name, middle initial. If military, show rank and branch of service. The name of the principal author is an absolute minimum requirement.

6. **REPORT DATE:** Enter the date of the report as day, month, year, or month, year. If more than one date appears on the report, use date of publication.

7a. **TOTAL NUMBER OF PAGES:** The total page count should follow normal pagination procedures, i.e., enter the number of pages containing information.

7b. **NUMBER OF REFERENCES:** Enter the total number of references cited in the report.

8a. **CONTRACT OR GRANT NUMBER:** If appropriate, enter the applicable number of the contract or grant under which the report was written.

8b, 8c, & 8d. **PROJECT NUMBER:** Enter the appropriate military department identification, such as project number, subproject number, system numbers, task number, etc.

9a. **ORIGINATOR'S REPORT NUMBER(S):** Enter the official report number by which the document will be identified and controlled by the originating activity. This number must be unique to this report.

9b. **OTHER REPORT NUMBER(S):** If the report has been assigned any other report numbers (either by the originator or by the sponsor), also enter this number(s).

10. **AVAILABILITY/LIMITATION NOTICES:** Enter any limitations on further dissemination of the report, other than those

imposed by security classification, using standard statements such as:

- (1) "Qualified requestors may obtain copies of this report from DDC."
- (2) "Foreign announcement and dissemination of this report by DDC is not authorized."
- (3) "U. S. Government agencies may obtain copies of this report directly from DDC. Other qualified DDC users shall request through \_\_\_\_\_."
- (4) "U. S. military agencies may obtain copies of this report directly from DDC. Other qualified users shall request through \_\_\_\_\_."
- (5) "All distribution of this report is controlled. Qualified DDC users shall request through \_\_\_\_\_."

If the report has been furnished to the Office of Technical Services, Department of Commerce, for sale to the public, indicate this fact and enter the price, if known.

11. **SUPPLEMENTARY NOTES:** Use for additional explanatory notes.

12. **SPONSORING MILITARY ACTIVITY:** Enter the name of the departmental project office or laboratory sponsoring (paying for) the research and development. Include address.

13. **ABSTRACT:** Enter an abstract giving a brief and factual summary of the document indicative of the report, even though it may also appear elsewhere in the body of the technical report. If additional space is required a continuation sheet shall be attached.

It is highly desirable that an abstract of classified reports be unclassified. Each paragraph of the abstract shall end with an indication of the military security classification of the information in the paragraph, represented as (TS), (S), (C), or (U).

There is no limitation on the length of the abstract. However, the suggested length is from 150 to 225 words.

14. **KEY WORDS:** Key words are technically meaningful terms or short phrases that characterize a report and may be used as index entries for cataloging the report. Key words must be selected so that no security classification is required. Identifiers, such as equipment model designation, trade name, military project code name, geographic location, may be used as key words but will be followed by an indication of technical context. The assignment of links, roles, and weights is optional.